ACS Macro Letters

Letter

pubs.acs.org/macroletters

Scattering from Colloid–Polymer Conjugates with Excluded Volume Effect

Xin Li,[†] Christopher N. Lam,[‡] Luis E. Sánchez-Díáz,[†] Gregory S. Smith,[†] Bradley D. Olsen,*[,‡] and Wei-Ren Chen*[,†]

[†]Biology and Soft Matter Division, Oak Ridge National Laboratory, Oak Ridge, Tennessee 37831, United States

[‡]Department of Chemical Engineering, Massachusetts Institute of Technology, Cambridge, Massachusetts 02139, United States

ABSTRACT: This work presents scattering functions of conjugates consisting of a colloid particle and a self-avoiding polymer chain as a model for protein–polymer conjugates and nanoparticle–polymer conjugates in solution. The model is directly derived from the two-point correlation function with the inclusion of excluded volume effects. The dependence of the calculated scattering function on the geometric shape of the colloid and polymer stiffness is investigated. The model is able to describe the experimental scattering signature of the solutions of suspending hard particle–polymer conjugates and provide additional conformational information. This model explicitly elucidates the link between the global conformation of a conjugate and the microstructure of its constituent components.

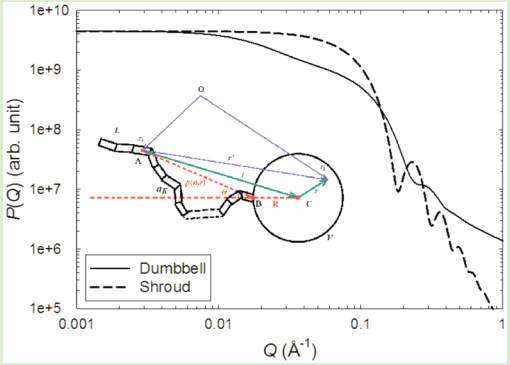

In recent years there has been much interest in developing multicomponent building blocks, such as colloid–polymer conjugates, to create programmed, novel functional materials that are thermodynamically favorable on both micro- and mesoscopic length scales.[1−5] The synthesis of these heterogeneous building blocks opens up unique opportunities to create new material combinations that hold promise for improving the performance and range of functionality accessible with self-organized materials.[6−11] For example, enzymes and globular proteins have catalytic properties and biological specificity that exceed those of synthetic materials. Incorporation of these proteins into protein–polymer conjugates has attracted significant interest to improve the pharmacokinetics of biological drugs, to produce biofunctional particles for targeted delivery of therapeutics,[12] and to self-assemble biofunctional nanomaterials such as catalysts.[13] Additionally, there has been significant interest in fullerene-polymer, polyhedral oligomeric silsesquioxane (POSS)-polymer, and nanoparticle–polymer conjugates for applications, such as molecular electronics, biosensors, and energy storage.[14,15]

To predict and control the self-assembly of these various colloid–polymer amphiphiles, it is important to understand the molecular configuration of individual molecules comprising the conjugate molecule. To this end, small angle scattering techniques[16] have been commonly used to investigate the conformation and positioning of a single colloid–polymer conjugate in these composites.[17−30] Various models of scattering functions have been proposed to extract quantitative structural characteristics from experiment. A composite power law approach has been used to separately obtain the qualitative structural features of colloid–polymer conjugates at different length scales reflected by the characteristic variations of scattering intensities at corresponding Q regimes.[19,20] Global scattering functions which provide unified conformational descriptions have also been proposed. A core–shell model was used to describe the scattering behavior of the systems in which the polymer chains as well as the associated solvent are treated as a homogeneous outer layer.[21,22] This simple model is unable to describe the scattering features originating from the microscopic structure. Alternatively, a mesoscopic approach which treats the polymer in the conjugates as an ideal Gaussian chain has been proposed.[23,24] However, in this model excluded volume effects within the polymer chain are not incorporated, and the correlation between a polymer chain and the colloid is calculated based on a phenomenological coarse-grain assumption that the polymer follows Gaussian statistics, with its center of mass located at a certain distance from the colloid. Therefore, it is expected that this model is unable to address the conformational features quantitatively for systems under good solvent conditions.[31] In this letter a small angle scattering function of a colloid–polymer conjugate with explicit incorporation of excluded volume effects is derived. This model is able to describe the experimental scattering features of colloid–polymer conjugates under good solvent conditions.

The conformation of a colloid–polymer conjugate can be expressed using the two-point spatial correlation function, often called the form factor

Received: October 31, 2014
Accepted: January 9, 2015
Published: January 13, 2015

ACS Publications © 2015 American Chemical Society

DOI: 10.1021/mz5006958
ACS Macro Lett. 2015, 4, 165−170

$$P_{\text{conjugate}}(Q) = \left\langle \sum_{i,j} \exp[-i\vec{Q}\cdot(\vec{r}_i - \vec{r}_j)] \right\rangle_{\vec{Q}} \quad (1)$$

where the brackets $\langle\ \rangle$ represent the average over all the molecular configurations and angular distribution of $\vec{Q}$, and $\vec{r}_i$ and $\vec{r}_j$ represent the positions of two scattering points.[16] For a colloid−polymer conjugate the positions $\vec{r}_i$ and $\vec{r}_j$ in eq 1 run through the whole system. Based on the physical locations of $\vec{r}_i$ and $\vec{r}_j$, $P_{\text{conjugate}}(Q)$ can be further expressed as

$$\begin{aligned} P_{\text{conjugate}}(Q) &= P_{\text{colloid}}(Q) + P_{\text{polymer}}(Q) \\ &\quad + P_{\text{colloid-polymer}}(Q) \\ &= \left\langle \sum_{i,j} \rho_i\rho_j \exp[-i\vec{Q}\cdot(\vec{r}_i - \vec{r}_j)] \right\rangle_{\vec{Q},\text{colloid}} \\ &\quad + \left\langle \sum_{i,j} b_i b_j \delta(\vec{r}_i)\delta(\vec{r}_j)\exp[-i\vec{Q}\cdot(\vec{r}_i - \vec{r}_j)] \right\rangle_{\vec{Q},\text{polymer}} \\ &\quad + \left\langle \sum_{i,j} b_i \delta(\vec{r}_i)\rho_j \exp[-i\vec{Q}\cdot(\vec{r}_i - \vec{r}_j)] \right\rangle_{\vec{Q},\text{colloid-polymer}} \end{aligned} \quad (2)$$

In eq 2, $P_{\text{colloid}}(Q)$, $P_{\text{polymer}}(Q)$, and $P_{\text{colloid-polymer}}(Q)$ represent the scattering contributions respectively from the intracolloid correlation, the intrapolymer correlation, and the colloid−polymer cross correlations, respectively. $\rho_{i,j}$ gives the scattering length density (SLD) at position $\vec{r}_{i,j}$ in the colloid particle, and $b_{i,j}$ is the total bound coherent scattering length of a Kuhn segment with its center at position $\vec{r}_{i,j}$ in the polymer chain.

The contributions from the first and second terms of eq 2 can be written as

$$P_{\text{colloid}}(Q) = (\rho V)^2 P_{\text{norm,colloid}}(Q) \quad (3)$$

$$P_{\text{polymer}}(Q) = \left(b\frac{L}{a_K}\right)^2 P_{\text{WLC}}(Q, L, a_K, R_{CS}) \quad (4)$$

where $\rho_{i,j}$ and $b_{i,j}$ reduce to ρ and b, respectively, with the assumption that the colloid and polymer are both homogeneous. Here V denotes the volume of a colloid particle, L the contour length of the polymer chain, a_K the Kuhn segment length, and R_{CS} the radius of the cross section of Kuhn segments. The prefactors $(\rho V)^2$ and $(bL/a_K)^2$ give the scattering ability of the colloid and polymer on an absolute intensity scale. $P_{\text{norm,colloid}}(Q)$ represents the normalized form factor for the colloid. Various mathematical forms have been derived for particles with different geometric shapes.[16] In colloid−polymer conjugates with a single polymer tether, the grafting density is low, and assuming that the polymer chain does not exhibit strong attractive or repulsive interactions with the colloid, the form factor of the polymer can be represented by $P_{\text{WLC}}(Q,L,a_K,R_{CS})$, which represents the scattering function for a worm-like chain (WLC) with excluded volume effects whose phenomenological expressions have been identified previously.[32,33] The third term on the right-hand side of eq 2 represents the cross correlation between the colloid and polymer. It can be further expressed as

$$\begin{aligned} &P_{\text{colloid-polymer}}(Q) \\ &= \left\langle \sum_{i,j} b_i\delta(\vec{r}_i)\rho_j \exp[-i\vec{Q}\cdot(\vec{r}_i - \vec{r}_j)] \right\rangle_{\vec{Q},\text{colloid-polymer}} \\ &= \left\langle 2b\rho \sum_{i=1}^{L/a_K} \delta(\vec{r}_i) \int_V d^3\vec{r}_j \exp[-i\vec{Q}\cdot(\vec{r}_i - \vec{r}_j)] \right\rangle_{\vec{Q},\text{colloid-polymer}} \\ &= 2b\rho \sum_{i=1}^{L/a_K} \delta(\vec{r}_i) \left\langle \int_V d^3\vec{r}' \exp[-i\vec{Q}\cdot\vec{r}'] \right\rangle_{\vec{Q},\text{colloid-polymer}} \\ &= 2b\rho \sum_{i=1}^{L/a_K} \delta(\vec{r}_i) \left\langle \int_V d^3\vec{r} \exp[-i\vec{Q}\cdot(\vec{r} + \vec{t})] \right\rangle_{\vec{Q},\text{colloid-polymer}} \\ &= 2b\rho \sum_{i=1}^{L/a_K} \delta(\vec{r}_i) \left\langle \exp(-i\vec{Q}\cdot\vec{t}) \int_V d^3\vec{r} \exp(-i\vec{Q}\cdot\vec{r}) \right\rangle_{\vec{Q},\text{colloid-polymer}} \\ &= 2b\rho \sum_{i=1}^{L/a_K} \delta(\vec{r}_i) \langle \exp(-i\vec{Q}\cdot\vec{t}) F_{\text{colloid}}(\vec{Q}) \rangle_{\vec{Q},\text{colloid-polymer}} \end{aligned} \quad (5)$$

where $\vec{r}'$ is the relative difference vector between the positions $\vec{r}_i$ and $\vec{r}_j$. It breaks into the sum of $\vec{t}$ and $\vec{r}$, where $\vec{t}$ is the relative vector from a point on the polymer to the geometric center of the colloid, and $\vec{r}$ is the relative coordinate within the colloid particle, as shown in Figure 1. Since the conjugate is not centrosymmetric, the integration over $\vec{t}$ has to be done numerically over all the Kuhn segments. A factor of 2 is assigned to take into account the fact that the two sampling points can be located at the polymer or the colloid with the same possibility. The volume integral

$$F_{\text{colloid}}(\vec{Q}) = \int_V d^3\vec{r} \exp(-i\vec{Q}\cdot\vec{r}) \quad (6)$$

gives the Q-dependent scattering amplitude of the colloid particle. $\vec{r}_i$ represents the center of a Kuhn segment which runs through the whole contour length L. Note that $\vec{r}_i$ is a discrete vector and eq 5 starting from the second equivalent sign is discretely summed over $\delta(\vec{r}_i)$ and is not a path integration. The relative vector $\vec{t}$ can be calculated based on the end-to-end

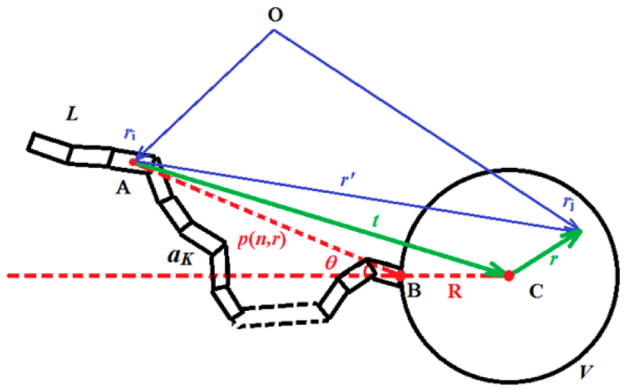

Figure 1. Schematic representation of a conjugate with a homogeneous spherical colloid (volume V, centered at C) and a wormlike chain (contour length L) attached to its surface at point B. A partial chain with n monomers follows the end-to-end distance distribution function $p(n,r)$. The red dashed lines indicate the azimuthal angle θ of the end of the partial chain to the axis defined by the attachment point and the center of the colloid. The colloid-chain cross term in the two-point correlation function (vector r_i and r_j) can be calculated numerically via the integral over n and θ.

DOI: 10.1021/mz5006958
ACS Macro Lett. 2015, 4, 165−170

distance distribution function $p(n,r)$ for a partial chain of n Kuhn segments at a radial distance r and a selected azimuthal angle θ. For an ideal Gaussian chain, $p(n,r)$ follows the Gaussian distribution. As a result, the scattering function takes the form of the Debye function.[34] Since the excluded volume effect is not incorporated, it is known that the Debye function underestimates the spatial correlation, especially at the high Q regime relevant to the intrachain correlation.[31] In our study, the mathematical expression of $p(n,r)$ proposed by des Cloizeaux is chosen because of its numerical accuracy as demonstrated by computer simulation with the inclusion of the intrachain excluded volume effect.[35,36] Here, $p(n,r)$ is an isotropic distribution, but in the conjugates, the colloid excludes the possibility of the polymer located within the scope of its volume. Considering this effect, the cross correlation between the polymer and colloid is evaluated numerically. However, the excluded volume effect caused by the colloid will also affect $p(n,r)$, the distribution of the polymer, which may be complicated but will not generate a qualitative difference. For the sake of simplicity, we assume that the mathematical form of $p(n,r)$ is the same as in the case of free chains but with part of the distribution excluded due to the volume of the colloid.

For a spherical colloid, the scattering amplitude takes the following expression

$$F_{\text{sphere}}(Q) = \frac{3V[\sin(QR) - QR\cos(QR)]}{(QR)^3} \tag{7}$$

where R is the sphere radius and V the volume ($V = (4\pi/3)R^3$). Since $F_{\text{sphere}}(Q)$ is an angle-independent real number, eq 5 can be further simplified to

$$\begin{aligned} &P_{\text{sphere-polymer}}(Q) \\ &= 2b\rho \sum_{i=0}^{L/a_K} \delta(\vec{r}_i) \frac{3V[\sin(QR) - QR\cos(QR)]}{(QR)^3} \\ &\quad \langle \exp(-i\vec{Q}\cdot\vec{t})\rangle_{\vec{Q},\text{sphere-polymer}} \\ &= 2b\rho \sum_{i=0}^{L/a_K} \delta(\vec{r}_i) \frac{3V[\sin(QR) - QR\cos(QR)]}{(QR)^3} \frac{\sin(Qt)}{Qt} \\ &= 4\pi b\rho \int_0^{L/a_K} \mathrm{d}n \int_0^{na_K} \mathrm{d}r \int_0^{\pi} \mathrm{d}\theta \sin(\theta) p(n,r) \\ &\quad \times \frac{3V[\sin(QR) - QR\cos(QR)]}{(QR)^3} \frac{\sin(Qt)}{Qt} \end{aligned} \tag{8}$$

where $((\sin(Qt))/Qt)$ results from the angular average of the kernel function $\exp(-i\vec{Q}\cdot\vec{t})$. The last equivalence expression is the transformation from a discrete spatial distribution of $\vec{r}_i$ to a continuous representation using spherical coordinates. In eq 8, the integral is explicitly expressed using the end-to-end distance distribution function $p(n,r)$.[35] The integration is performed numerically using the trapezoidal method in MATLAB.[37]

In Figure 2 we present the form factor $P(Q)$ calculated from eqs 2−8 for the hard sphere−polymer conjugates. The conformational parameters R, L, a_K, and R_{CS} used in the calculation are 20, 2667, 10, and 2 Å, respectively, values representative of a globular protein conjugated to a long polymer chain with a similar total scattering power. The SLDs of the sphere and polymer are both chosen to be 2.52×10^{-6} Å^{-2}, the same as the SLD of lysozyme, so that the total scattering length of the sphere and polymer are equal. The number density of the colloid−polymer conjugate is assigned to be 4.29×10^{17} cm^{-3}, which corresponds to 1% (w/v) aqueous solution of lysozyme. Therefore, the calculated scattering profile can be presented in the unit for absolute intensity in

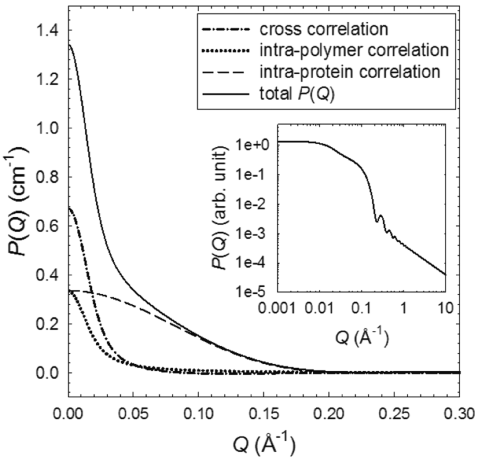

Figure 2. $P(Q)$ of a sphere−polymer conjugate calculated following eqs 2−8 and shown on a linear scale. The solid line is the total scattering of $P(Q)$, including the contributions from the intrapolymer correlation (dotted), the intracolloid correlation (dashed) and the cross correlation between the colloid and polymer (dash-dotted). The inset shows the total $P(Q)$ plotted on a logarithmic scale.

Figures 2−5. The cross contribution between the colloid and the polymer is negative at some Q values because of the phase

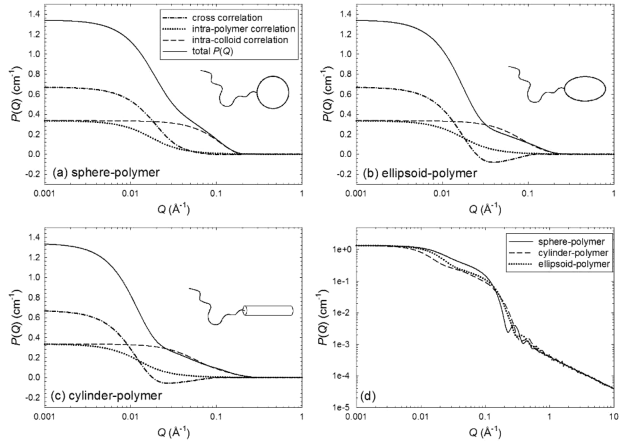

Figure 3. $P(Q)$s of (a) sphere-polymer, (b) ellipsoid-polymer and (c) cylinder-polymer conjugates, with intracolloid (dashed), intrapolymer (dotted), cross (dash-dotted), and total (solid) correlations shown separately. The comparison of the total $P(Q)$s for these three cases is presented in panel (d) on a logarithmic scale.

interference in the spatial correlation. Therefore, for the sake of clarity, the $P(Q)$s are shown on a linear scale for the y-axis. Since the total scattering lengths of the colloid and the polymer are the same, the total scattering intensities and the zero-angle intensities of the intracolloid (dashed line) and intrachain (dotted line) correlations are identical. Since the polymer chain is more loosely packed than the colloid, it spreads over a larger spatial distance, and its Guinier region is located at lower Q.[16] In the intermediate Q region (Q = 0.05−0.2 Å^{-1}), the scattering function is dominated by the contribution from the colloid particle. On the other hand, in the high Q region ($Q > 1$ Å^{-1}), $P(Q)$ is dominated by the intrapolymer correlation due to its slower decay. It should be noted that the summation of the three terms in eq 2 gives the extra concave shape of $P(Q)$ close to the position where the cross correlation and the intracolloid correlation are equal, for example, Q = 0.02−0.05 Å^{-1} in Figure

DOI: 10.1021/mz5006958
ACS Macro Lett. 2015, 4, 165−170

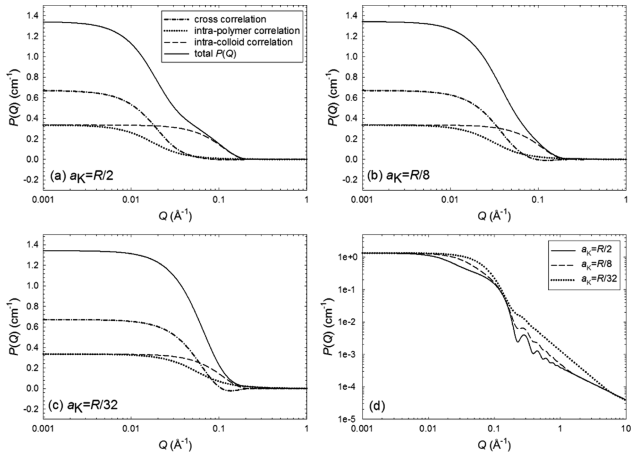

Figure 4. $P(Q)$ of a sphere-polymer conjugate calculated as a function of the Kuhn length a_K. The contour length L is fixed at 2667 Å and the sphere radius at 20 Å. The Kuhn lengths are (a) a_K = 10, (b) 2.5, and (c) 0.625 Å, and their $P(Q)$s are compared in panel (d).

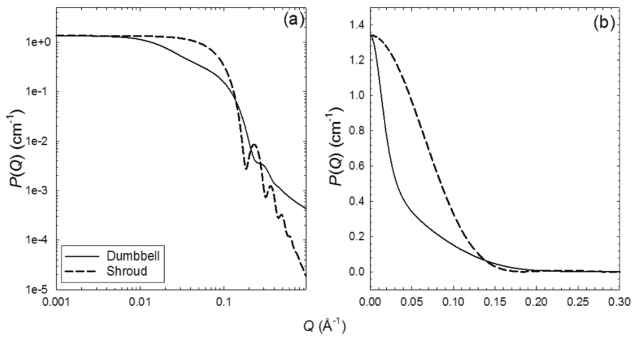

Figure 5. $P(Q)$s of the dumbbell (solid) and shroud models (dashed) of a sphere−polymer conjugate, shown on a (a) logarithmic (a) and a (b) linear scale. In the shroud model, the polymer is assumed to be fully wrapped around the spherical colloid.

2. This is a specific feature of the scattering profile for colloid−polymer conjugates that cannot be described using the previous approaches.[17−30]

It is important to highlight additional insightful information provided by our calculation. For example, existing scattering spectra of colloid−polymer conjugates,[26−30] with similar conformational parameters used in the calculations presented in Figure 2, are seen to be characterized by an upturn in the Q range of 0.01−0.05 Å^{-1}. As demonstrated by eq 5, because of the scattering contribution from the colloid−polymer, the cross correlation is twice that of the intracolloid and intrachain correlations; therefore, the zero-angle intensity of the entire system is dominated by its contribution (dash-dotted line). Our calculations show that the experimentally observed upturn could result from the intraconjugate cross correlation between the colloid and the polymer instead of the formation of interconjugate aggregates or other large length scale heterogeneous structures.

The calculation of colloid−polymer conjugate form factors can be further extended to investigate colloids with different geometric shapes such as ellipsoids and cylinders, corresponding to various shapes of proteins or peptides in bioconjugate materials. The scattering functions of conjugates consisting of a sphere, ellipsoid, or cylinder with a polymer are calculated via eqs 2−6. The results are given in panels (a), (b), and (c) of Figure 3, respectively. Their schematic representations are given in the inset of each panel, and the comparison of their total scattering functions is given in panel (d). The parameters used in the calculations are a sphere of radius 20 Å, an ellipsoid with a long axis of 40 Å and short axes of 14.14 Å, a cylinder of radius 11 Å and length 88 Å, and the parameters for the polymer are the same as in Figure 2. The volume and total scattering length for the three different colloids are identical. From sphere to ellipsoid to cylinder, the colloid is elongated in the radial direction and contracted in the axial direction, causing the Guinier region of the scattering profile due to the colloid (dashed curve in panels (a)−(c)) to extend toward lower values of Q, and the same trend is observed in the total scattering profile of the conjugates, clearly shown in panel (d). Consequently, the concave region in the total $P(Q)$ near Q = 0.03 Å^{-1} becomes progressively more pronounced upon increasing the aspect ratio. The oscillation in the calculated total $P(Q)$ of a conjugate also exhibits a strong dependence on the geometric shape of its constituent colloid. For example, due to the large aspect ratio of the cylinder, two sets of oscillations at Q = 0.006−0.1 Å^{-1} and 0.5−2 Å^{-1} originating from the correlation along the axial and radial directions, respectively, are observed in our calculations given in panels (c) and (d).

Many different chemical and physical stimuli can modulate the conformation of polymer chains; therefore, it is important to understand the dependence of the scattering function on the stiffness of the polymer chain. For a flexible polymer chain, the ratio $N = L/a_K$ characterizes the stiffness of the polymer chain. A polymer with a larger value of N is characterized by more flexible conformations.[34] From panel (a) to (c) of Figure 4, the Kuhn length decreases from $a_K = R/2$ to $a_K = R/32$, which reflects a deteriorating solvent condition. The intrapolymer correlation shifts toward high Q due to a smaller Kuhn length and the contraction of the global size of the polymer. As a result, the aforementioned concave region in the $P(Q)$ curve becomes less discernible. In the high Q range (Q > 0.2 Å^{-1}) the intrapolymer scattering contribution (dotted line in panels (a)−(c)) weighs more in the total $P(Q)$, and the oscillations from the intracolloid correlation are progressively masked by the intrapolymer correlation (panel (d)). As demonstrated in panel (d), $P(Q)$ decays faster in the Porod region (Q > 0.8 Å^{-1}) with a smaller a_K due to the more compact polymer conformation. Meanwhile, the first minimum of the oscillations (Q = 0.15−1 Å^{-1}) is seen to shift toward low Q, indicating the size of the colloid increases due to the collapsed polymer attached onto its surface.

An important question regarding the conformation of colloid−polymer conjugates is whether the polymer chain wraps around the colloid to create a shield (shroud model) or exists as a relatively unperturbed flexible chain attached to the colloid (dumbbell model). In the former scenario, the polymer may enshroud the protein due to the presence of strong enthalpic interactions between colloid and polymer or in conjugates where the polymer size substantially exceeds that of the colloid; in the latter case, if there are weak interactions between a colloid and polymer of similar size, it is more favorable for the polymer to adopt a coil configuration extended away from the colloid due to the large entropic penalty of wrapping around the colloid.[17] In the extreme case of a shroud model, one can assume that the polymer chain fully collapses on the surface of the colloid, which gives a sphere twice the volume of the spherical colloid in the conjugate. The form factor of this shroud limit is shown in Figure 5 as the

DOI: 10.1021/mz5006958
ACS Macro Lett. 2015, 4, 165−170

dashed line and compared to the sphere-polymer conjugate form factor as the solid line, where the colloid and polymer are assumed to have the same SLD in this comparison. Colloid–polymer conjugates that adopt a shroud configuration in which the SLDs of the colloid and polymer are different form a core–shell structure. While the form factor of a core–shell structure will depend upon the relative difference between the SLDs of the component blocks and that of the solvent, the form factor will remain qualitatively similar to that of a shroud configuration in which the SLD is homogeneous. The SANS instrument resolution function has been taken into account, which has smeared the oscillations in the high Q region ($Q > 0.1$ Å^{-1}), but the decay of its intensity can certainly be used to deduce the conformational characteristics of a colloid–polymer conjugate in solution. The shroud model decays much faster, closer to a power law of −4, than the dumbbell model. The concave section of $P(Q)$ at $Q = 0.03$ Å^{-1}, originating from the cross correlation, is another feature which can be used for characterization of the conjugate conformation.

It is instructive to briefly discuss the influence of polydispersity, which is caused by the size distribution of the constituent polymer or colloid, on the calculated scattering functions. Using a sphere–polymer conjugate as an example, this effect can be incorporated through the following equations:[38]

$$P(Q) = \int f(R, L) P_{\text{sphere-polymer}}(Q, R, L, a_K, R_{CS}) \mathrm{d}R\mathrm{d}L \tag{9}$$

where $f(R,L)$ is the probability density function for the distribution of R and L under the constraint of the following normalization criterion:

$$\int f(R, L) \mathrm{d}R\mathrm{d}L = 1 \tag{10}$$

The polydispersity of the colloid–polymer conjugates will smear some of the features in the scattering profiles such as the minima and maxima, which is similar to the effect of polydispersity on the scattering of spherical colloids.

To summarize, we present a theoretical model for the scattering function of colloid–polymer conjugates. This model is directly derived from the two-point spatial correlation function with the incorporation of the excluded volume effect with valid approximations. The scattering functions calculated from this model, in the future, will be used to analyze the experimentally observed scattering features of the colloid–polymer conjugates and provide additional insightful interpretations that are not intuitively obvious. This model facilitates the quantitative conformational investigation of colloid–polymer conjugates using scattering.

AUTHOR INFORMATION

Corresponding Authors

* E-mail: bdolsen@mit.edu.

*E-mail: chenw@ornl.gov.

Notes

The authors declare no competing financial interest.

ACKNOWLEDGMENTS

This work was supported by the U.S. Department of Energy, Office of Science, Office of Basic Energy Sciences, Materials Sciences and Engineering Division, and by the Scientific User Facilities Division, Office of Basic Energy Sciences, U.S. Department of Energy.

REFERENCES

(1) Jones, R. A. L. *Soft Condensed Matter*; Oxford University Press: Oxford, 2002.

(2) Zhang, W.-B.; Yu, X.; Wang, C.-L.; Sun, H.-J.; Hsieh, I.-F.; Li, Y.; Dong, X.-H.; Yue, K.; Van Horn, R.; Cheng, S. Z. D. *Macromolecules* **2014**, *47*, 1221.

(3) Boyer, C.; Huang, X.; Whittaker, M. R.; Bulmus, V.; Davis, T. P. *Soft Matter* **2011**, *7*, 1599.

(4) Hoffman, A. S.; Stayton, P. S. *Prog. Polym. Sci.* **2007**, *32*, 922.

(5) Stayton, P. S.; Shimoboji, T.; Long, C.; Chilkoti, A.; Chen, G.; Harris, J. M.; Hoffman, A. S. *Nature* **1995**, *378*, 472.

(6) Boerakker, M. J.; Hannink, J. M.; Bomans, P. H. H.; Frederik, P. M.; Nolte, R. J. M.; Meijer, E. M.; Sommerdijk, N. A. J. M. *Angew. Chem., Int. Ed.* **2002**, *41*, 4239.

(7) Boerakker, M. J.; Botterhuis, N. E.; Bomans, P. H. H.; Frederik, P. M.; Meijer, E. M.; Nolte, R. J. M.; Sommerdijk, N. A. J. M. *Chem.—Eur. J.* **2006**, *12*, 6071.

(8) Dirks, A. J.; Nolte, R. J. M.; Cornelissen, J. J. L. M. *Adv. Mater.* **2008**, *20*, 3953.

(9) Velonia, K.; Rowan, A. E.; Nolte, R. J. M. *J. Am. Chem. Soc.* **2002**, *124*, 4224.

(10) Hassouneh, W.; Fischer, K.; MacEwan, S. R.; Branscheid, R.; Fu, C. L.; Liu, R.; Schmidt, M.; Chilkoti, A. *Biomacromolecules* **2012**, *13*, 1598.

(11) Olsen, B. D. *Macromol. Chem. Phys.* **2013**, *214*, 1659.

(12) Greenwald, R. B.; Choe, Y. H.; McGuire, J.; Conover, C. D. *Adv. Drug Delivery Rev.* **2003**, *55*, 217.

(13) Amaya, T.; Saio, D.; Hirao, T. *Tetrahedron Lett.* **2007**, *48*, 2729.

(14) Ren, X.; Sun, B.; Tsai, C.-C.; Tu, Y.; Leng, S.; Li, K.; Kang, Z.; Van Horn, R. M.; Li, X.; Zhu, M.; Wesdemiotis, C.; Zhang, W.-B.; Cheng, S. Z. D. *J. Phys. Chem. B* **2010**, *114*, 4802.

(15) Zhang, Z.; Horsch, M. A.; Lamm, M. H.; Glotzer, S. C. *Nano Lett.* **2003**, *3*, 1342.

(16) *Neutron, X-rays and Light. Scattering Methods Applied to Soft Condensed Matter*; Lindner, P., Zemb, Th., Eds.; North-Holland: Amsterdam, 2002.

(17) Pai, S. S.; Hammouda, B.; Hong, K.; Pozzo, D. C.; Przybycien, T. M.; Tilton, R. D. *Bioconjugate Chem.* **2011**, *22*, 2317.

(18) He, L.; Wang, H.; Garamus, V. M.; Hanley, T.; Lensch, M.; Gabius, H.-J.; Fee, C. J.; Middelberg, A. *Biomacromolecules* **2010**, *11*, 3504.

(19) Morfin, I.; Buhler, E.; Cousin, F.; Grillo, I.; Boué, F. *Biomacromolecules* **2011**, *12*, 859.

(20) Frisman, I.; Orbach, R.; Seliktar, D.; Bianco-Peled, H. *J. Mater. Sci: Mater. Med.* **2010**, *21*, 73.

(21) Castelletto, V.; Krysmann, M. J.; Clifton, L. A.; Lambourne, J. *J. Phys. Chem. B* **2007**, *111*, 11330.

(22) Lu, Y.; Harding, S. E.; Turner, A.; Smith, B.; Athwal, D. S.; Grossmann, J. G.; Davis, K. G.; Rowe, A. J. *J. Pharm. Sci.* **2008**, *97*, 2062.

(23) Lund, R.; Shu, J.; Xu, T. *Macromolecules* **2013**, *46*, 1625.

(24) Shu, J. Y.; Lund, R.; Xu, T. *Biomacromolecules* **2012**, *13*, 1945.

(25) Frisman, I.; Shachaf, Y.; Seliktar, D.; Bianco-Peled, H. *Langmuir* **2011**, *27*, 6977.

(26) Maccarini, M.; Briganti, G.; Rucareanu, S.; Lui, X.-D.; Sinibaldi, R.; Sztucki, M.; Lennox, R. B. *J. Phys. Chem. C* **2010**, *114*, 6937.

(27) Svergun, D. I.; Ekström, F.; Vandegriff, K. D.; Malavalli, A.; Baker, D. A.; Nilsson, C.; Winslow, R. M. *Biophys. J.* **2008**, *94*, 173.

(28) Jackson, A.; White, J. *Physica B* **2006**, *385–386*, 818.

(29) Hamley, I. W.; Krysmann, M. J. *Langmuir* **2008**, *24*, 8210.

(30) Krysmann, M. J.; Funari, S. S.; Canetta, E.; Hamley, I. W. *Macromol. Chem. Phys.* **2008**, *209*, 883.

(31) Schurtenberger, P. In *Neutron, X-rays and Light. Scattering Methods Applied to Soft Condensed Matter*; Lindner, P., Zemb, Th., Eds.; North-Holland: Amsterdam, 2002.

DOI: 10.1021/mz5006958
ACS Macro Lett. 2015, 4, 165–170

(32) Pedersen, J. S.; Schurtenberger, P. *Macromolecules* **1996**, *29*, 7602.
(33) Chen, W.-R.; Butler, P. D.; Magid, L. J. *Langmuir* **2006**, *22*, 6539.
(34) Teraoka, I. *Polymer Solutions*; Wiley-Interscience: New York, 2001.
(35) des Cloizeaux, J. *J. Phys. (Paris)* **1981**, *42*, 635.
(36) Valleau, J. P. *J. Chem. Phys.* **1996**, *104*, 3071.
(37) Butt, R. *Introduction to Numerical Analysis Using MATLAB*; Jones and Bartlett Publishers: Sudbury, 2010.
(38) Pedeesen, J. S. In *Neutron, X-rays and Light. Scattering Methods Applied to Soft Condensed Matter*; Lindner, P., Zemb, Th., Eds.; North-Holland: Amsterdam, 2002.

DOI: 10.1021/mz5006958
ACS Macro Lett. 2015, 4, 165−170